Type of contribution:
Editorial
Research Paper
Case Study
▶ Review Paper
Scientific Data
Report of Tech. Application

mesi e-issn. 2798-5245

Mechanical Engineering for Society and Industry
Vol. 6, No. 2 (2026) pp 298-316
https://doi.org/10.31603/mesi.14790

Review on effect of Interpass temperature for wire arc additive manufacturing process

Nor Ana Rosli[1,3*], Mohd Rizal Alkahari[2,3], Mohd Hadzley Abu Bakar[1], Lailatul Harina Paijan[1], Mohd Syafiq Abd Aziz[2], Mohamad Nordin Mohamad Norani[4]

[1] Faculty of Industrial and Manufacturing Technology and Engineering, Universiti Teknikal Malaysia Melaka (UTeM), Hang Tuah Jaya, 76100 Durian Tunggal, Melaka, **Malaysia**
[2] Faculty of Mechanical Technology and Engineering, Universiti Teknikal Malaysia Melaka (UTeM), Hang Tuah Jaya, 76100 Durian Tunggal, Melaka, **Malaysia**
[3] Centre for Advanced Research on Energy (CARe), Universiti Teknikal Malaysia Melaka (UTeM), Hang Tuah Jaya, 76100 Durian Tunggal, Melaka, **Malaysia**
[4] Faculty of Engineering, Built Environment, and Information Technology, MAHSA University, **Malaysia**
✉ ana@utem.edu.my

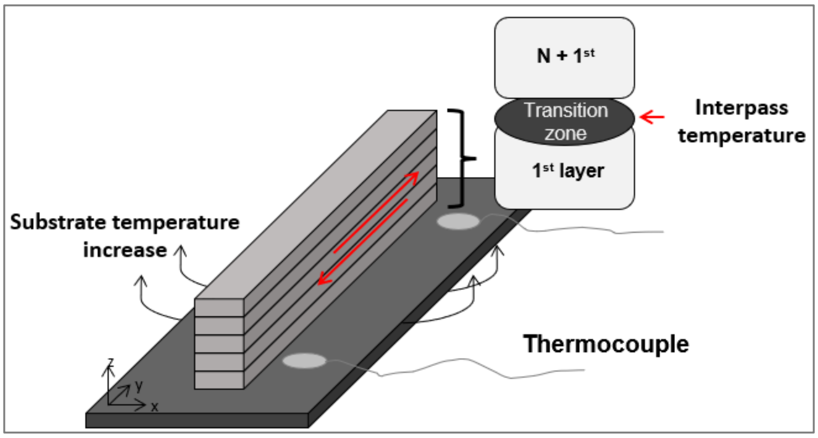

Highlights:

- This review systematically examines the role of interpass temperature (15–600 °C) in controlling heat accumulation and geometrical distortion in WAAM processes.
- Interpass temperature is identified as a critical but under-standardized parameter governing macrostructure, microstructure, and mechanical performance across different materials.
- Comparative analysis reveals material-dependent interpass temperature effects, highlighting inconsistencies and limitations in existing experimental and modeling approaches.
- Key research gaps are identified, emphasizing the need for integrated thermal–process control frameworks to enable accurate and repeatable WAAM fabrication.

Abstract

Wire Arc Additive Manufacturing (WAAM) enables the efficient fabrication of large metal components through high deposition rates. The process offers notable advantages, including the ability to produce complex geometries and reduce overall manufacturing costs. However, forming accuracy remains a major limitation. The layer-by-layer deposition approach in WAAM often leads to geometrical distortion, which negatively impacts dimensional accuracy and surface quality. Therefore, this review focuses on the influence of interpass temperature in range from 15 °C to 600 °C for controlling the heat accumulation and improving dimensional accuracy. The effects of interpass temperature on macrostructure, microstructure, and mechanical properties are critically discussed in various materials. The findings reveal that, despite its significant impact on build quality, standardized interpass temperature guidelines and material-specific optimization strategies remain limited, highlighting the need for systematic investigations and integrated thermal–process control frameworks in future WAAM research.

Keywords: Additive manufacturing; Wire arc additive manufacturing; Interlayer temperature; Heat accumulation

Article info
Submitted: 2025-09-12
Revised: 2026-01-20
Accepted: 2026-02-04

Publisher
Universitas Muhammadiyah Magelang

1. Introduction

Additive manufacturing (AM) is a cutting-edge technology that allows for customised shape and on-demand production with minimal human intervention. The AM technology is an automated process, creates components directly from computer-aided design (CAD) data, without the necessity for conventional tools, jigs, or fixtures [1]. According to ASTM standards, AM is defined as the process of joining materials to produce parts directly from 3D data by adding layers of material, in contrast to the conventional subtractive manufacturing method [2], [3], [4]. AM offers numerous benefits, including enhanced design freedom, decreased production durations, and minimised waste [5], [6], [7]. Due to these benefits, AM technology has gained applications in various sector, including biomedical, aerospace, marine, and construction [8], [9]. The seven primary categories of AM methods, as defined by ASTM, are stereolithography (SLA), material jetting (MJ), material extrusion (ME) , binder jetting (BJ), powder bed fusion (PBF), sheet lamination (SL), and direct energy deposition (DED) [10], [11]. AM technology has evolved from prototype to wider applications in modelling, tooling, and manufacturing. Three materials commonly used in additive manufacturing are polymers, ceramics, and metals. All seven categories encompass the use of these materials. Additionally, some additive processes are more suitable for specific materials than others.

Wire Arc Additive Manufacturing (WAAM), a specific form of the DED method, utilizes arc welding as its heat source to deposit materials in a layered fashion [12]. In the WAAM process, wire is used as the feedstock, where a consumable wire is continuously fed and deposited using an electric arc and builds layer by layer. The WAAM process is integrated with conventional arc welding such as GMAW [13], GTAW, and PAW. GMAW-based WAAM process enables high deposition rates while GTAW and PAW offer independent control of heat input and wire feed speed [14].

WAAM has received more attention in industry and academia for manufacturing metal parts due to its advantages in deposition rate, design freedom, and buy to fly ratio. According to Scopus databases, there are 2855 articles for the keywords "wire arc additive manufacturing" after limit subject area to engineering. The graph shows a remarkable increase across the year, as shown in **Figure 1**.

However, development of WAAM especially on interpass temperature is remain underexplored. Issue on heat accumulation present during deposition is critical challenge that affect the properties of fabricated components. Therefore, the study presents a critical review of WAAM in its heat accumulation aspects of develop components. The review works start with the introduction of AM, next briefly discuss WAAM process and narrow down the discussion on effect of interpass temperature on macrostructure, microstructure and mechanical properties.

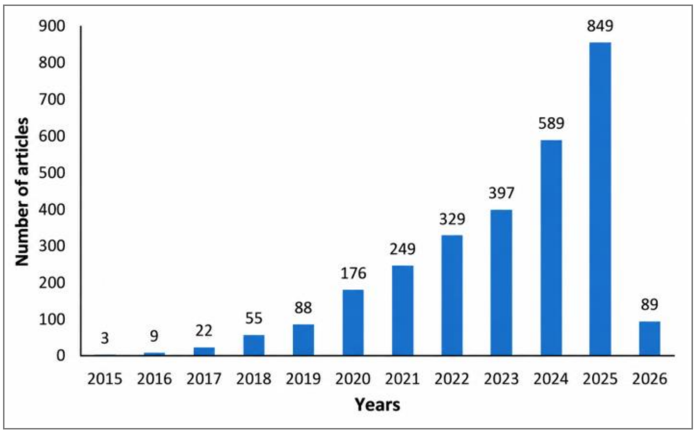

Figure 1. Increasing trend publication of WAAM process

2. Wire Arc Additive Manufacturing

The WAAM process's significant promise in fabricating metal parts lies in the use of an electric arc as the heat source that allows large-scale component deposition [15], [16]. WAAM method also is classified as multi-pass arc welding-based AM technology in manufacturing metallic components. WAAM process also significantly outperform in terms of cost than powder-based method. This may be seen in the amount of energy used, the cost of production, including the cost of raw materials, and the dimensions of the component are not just limited to the size of the printing cell [17]. Despite the obvious benefits of the WAAM process, there are still a lot of significant obstacles to overcome in terms of variability and uncertainty of the mechanical characteristics. **Figure 2** depicts the top fifteen research institutions worldwide that have published the most articles on the WAAM technique, and the University of Wollongong is the top on the list.

WAAM has distinct merits in fabricating metallic components compared to other metallic AM processes. Despite its benefits, the WAAM process still faces challenges due to complex thermal issues and heat accumulation, which are substantially impacting the fabricated components' properties and the microstructure evolution. The WAAM technique with a layer-by-layer structure imposes consecutive heating and cooling cycles on the previously solidified beads during the manufacturing process. Consequently, considerable heat applied to the workpiece will result in severe thermal damage such as residual stresses, significant distortions, and structural collapse. The issues with heat accumulation and complex thermal history restricted the application of the WAAM process due to the difficulty to control the dimensional accuracy, microstructure evolution, deposition flaws and mechanical properties of fabricated parts [18], [19], [20]. Therefore, regulating the cooling rate during the welding process to achieve the appropriate microstructure is critical since excessive cooling will result in the formation of additional ferrites. According to Vahedi *et al*. [21] the microstructure is strongly influenced by the temperature cycle that the material undergoes during the fabrication process. However, the increasing number of layers is becoming more complicated to cool through conduction. Heat dissipation at the top layer reduces heat accumulation and heat transfer to the lower layers. The key concern is the heat accumulation that affects the cooling rate and thermal cycle of the newly deposited and previously deposited layers, resulting in microstructural changes [22]. The interpass temperature control is a practical approach to realising and maintaining the thermal boundary condition during subsequent layer deposition. The significance of interpass temperature control in the WAAM process has been reported in numerous studies. However, the process control based on interlayer should be carefully selected because it relates to the surface unevenness and temperature supply. The higher the interlayer temperature, the longer it takes to cool down because the temperature component is kept at a high level throughout the manufacturing process. Furthermore, conventional weld seams suggested that monotonic strength of tensile and yield tends to be reduced when the interlayer temperature is low, and the cooling rate is high. Therefore, it is expected that increasing the interlayer temperature will result in a stronger bond between the different layers and a low distortion or residual stress. Choosing the right interpass temperature is a time consuming and challenging task. Thus, this study conducts a review on the effect of the interpass temperature in the WAAM process.

Figure 2. Top 15 research institutes with number of documents related to the WAAM process

3. Controlled Interpass Temperature

The temperature difference of the weld area in between successive welding passes is referred to as the interpass temperature. Maintaining an appropriate interpass temperature is vital to cooling rate to ensure the desired metallurgical structure and mechanical properties of the welded joint. **Figure 3** shows the illustration of the interpass temperature control. The ASTM F3187-16 standard guide indicates that the interpass temperature is essential for the DED process and materials [23]. The interpass temperature in the multipass weld is defined by the welding standard AWS A3.0 as the temperature of the weld area between weld passes [24]. Optimisation of heat input, interpass temperature, cooling rate, suitable consumable selection, defect-free joints, and rapid productivity is required to meet the demand for high productivity [25], [26], [27]. Thus, the component quality should fulfil the operation requirement before deployment in the AM technology.

In the WAAM process, the geometrical and mechanical properties of deposited components are directly affected by the welding condition and the deposited material. In addition, the welding process always results in the heat treatment of the surrounding material deposition, which affects the current and adjacent layers [28]. Since heat transmission impacts the cooling rate and thermal cycle of the earlier and currently deposited layers. As result, the component's insufficient heating-cooling process leads to inferior quality and performance of the fabricated parts. According to Bintao Wu *et al*. [29] heat accumulation reduces the geometrical accuracy of components manufactured using the WAAM process. WAAM manufacturing is necessary to achieve the solidification microstructure, including grain size and shape. Thus, it is essential to understand the underlying process and to optimise the microstructural control. In the recent years, there has been a significant interest in the WAAM process's interpass temperature. **Table 1** summarizes studies on the effects of interpass temperature using materials such as duplex stainless steel, mild steel, Al alloys, Ti6Al4V, Inconel 625, and others. Interpass temperatures ranged from ambient to 800 °C, typically in 100–400 °C increments. These studies highlight correlations between interpass temperature and macrostructure, microstructure, and mechanical properties.

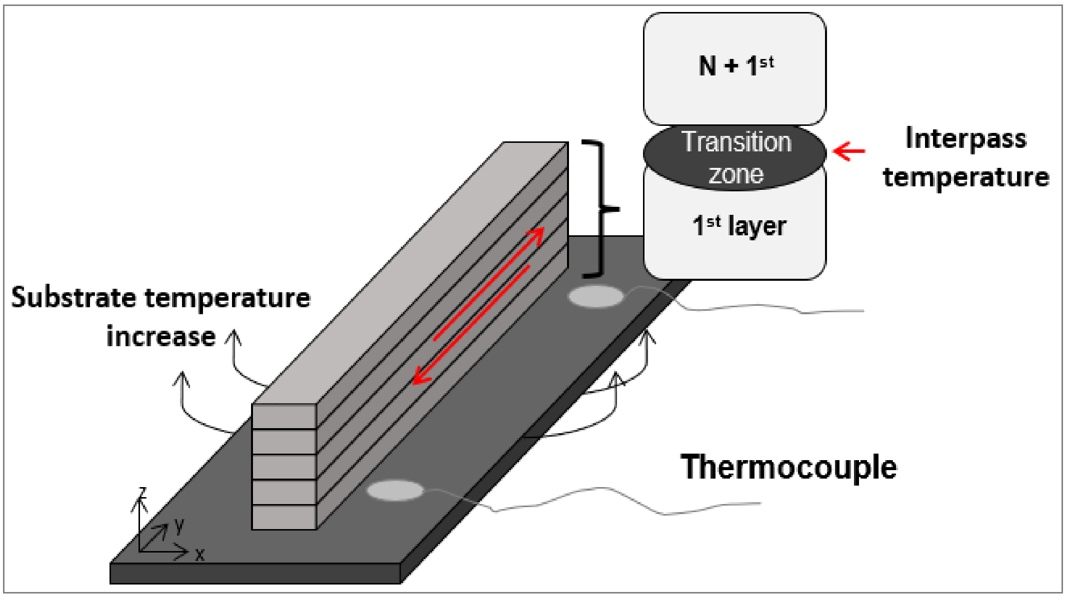

Figure 3. Schematic of interpass temperature control in layer by layer deposition

4. Effect of Interpass Temperature on the Surface Morphologies

During deposition, the surface morphologies also experience increased temperatures and the effect of interpass temperature. Several researchers discussed the impact of interpass temperature, which is one of the ways to control the microstructure caused by the thermal cycle encountered during the WAAM process. For example, Guo Y *et al*. [20] studied the forming features, the thermal cycle, the evolution of the microstructure and the mechanical properties of samples fabricated with the WAAM process. As a result, owing to the heat input, the bead width expanded rapidly as the interpass temperature increase. A similar finding from other researchers demonstrated narrow width at the first layer deposition and experienced a sharp rise in the first few layers as the interpass temperature increased [18], [22], [30], [31], [32]. Wu *et al*. [29] found that the height of the deposited wall decreased by 11.7%, while its width increased by 12.2% when the interpass temperature raised from 100 °C to 300 °C [31]. Ren *et al*. [30] discovered the width of the deposited wall reduced by 14.6%, 26.9% and 29.3%, and the layer height increased by 11.9%, 23.8%, and 26.2% when the interpass temperature was decreased from 200 °C to 160 °C, 120 °C, and 80 °C, respectively. Guo D *et al*. [33] and Shalini Singh *et al*. [34] also found that the width of samples gradually increases when interpass temperature increases, and in contrast to the average height displayed as shown in **Figure 4**. This finding indicated that the cooling rate decreased as the interpass temperature increased. Moreover, as the cooling rate decreased, the deposited parts' height decreased, and the width increased. Besides, greater heat input might influence when interpass temperature increases and becomes more melting on previous layers, resulting in flatter and wider deposition [34]. Overall, the study outcome indicated that the interpass temperature significantly impacted the component geometry even when other process variables such as the layer height were kept constant.

Table 1. Primary studies

Year	Process	Material	Interpass	Key area	Aim of the study	Refs.
2017	GTAW	5A06 Aluminium Alloy	-	Theoretical model	Develop a theoretical model to determine the appropriate interpass temperature	[35]
2017	GTAW	Fe_3Al	280 °C, 320 °C, 360 °C, and 400 °C	Effect of interpass temperature	Determine the influence of deposition current and interpass temperature on build-up wall properties.	[32]
2018	GTAW	Ti6Al4V	200 °C		The study maintains the process interpass temperature below 200 °C and examines heat accumulation's influence on targeted deposition.	[29]
2018	GTAW	Ti6Al4V	100 °C, 200 °C and 300 °C	Improvement-force interpass cooling	Understanding the influence of interpass cooling on the material deposition and implementing force interpass cooling to improve material properties	[31]
2018	GMAW	ER70S-6	-	Simulation-schedule deposition interlayer idle time	Utilise FE simulation to monitor the cooling of each layer immediately upon deposition and determine the required idle time to achieve the desired interpass temperature.	[36]
2018	GMAW	Mild steel	-	Compare effect interpass and numerical result	Investigate the effect of the deposition process on the deposition shape numerically.	[37]
2019	CMT-Adv	Al-6.3 Mg Alloy	200 °C, 160 °C, 120 °C, and 80 °C	Effect of interpass temperature	Study the effect of various interpass temperatures and control the dwell time between layer deposition	[30]
2019	GMAW	Duplex stainless steel	150 °C and 250 °C		Determine the correlation between the rate of heat input and the temperature of the interlayer considering thermal cycles and microstructures.	[38]
2019	GMAW	ER110S	800 °C to 500 °C		Investigate the complex thermal history of the WAAM process and the critical role of cooling rate control.	[22]
2020	GMAW	Duplex stainless steel	50 °C, 100 °C and 150 °C		Explore how interlayer temperature and processing period interact with product structure.	[39]
2020	GMAW	Mild steel	150 °C	Effect of interpass with CO_2 forced interpass cooling	Determine the efficiency of interpass temperature regulation and forced interpass cooling.	[40]
2020	CMT	ER5356 Al alloy	-	Four different cooling process	Investigate the interlayer, and online vortex cooling affect the deposited wall morphology, microstructure, and mechanical characteristics.	[41]

Table 1. (Continous)
Primary studies

Year	Process	Material	Interpass	Key area	Aim of the study	Refs.
2020	GMAW	Mild steel	150 °C and 300 °C	Effect of interpass temperature	The study Investigate the influence of interlayer temperature on the strength of the material and residual stress within manufactured material.	[42]
2020	GMAW	Ti6Al4V	15 °C		Determine the cooling rate of deposited materials with Interpass temperature control.	[43]
2020	Pulse CMT	Al-5356	125 °C		Examine the effect of temperature and heat accumulation on component qualities that contribute to geometry creation and mechanical properties.	[28]
2020	Pulse GMAW/ CMT	ER5183	50 °C and 100 °C		Investigate the effects of heat input, interlayer temperature, and interlayer dwell time on porosity formation and distribution under different deposition conditions.	[44]
2020	Pulsed GMAW	ER5356	50 °C and 100 °C		Study the impact of varying the interpass temperature on the porosity content and mechanical properties of WAAM parts.	[45]
2020	GMAW	ER70S-6	250 °C	Different idle time and Implemented air jet impingement	Air-jet impingement on deposited material was used to boost convective heat transfer rate.	[46]
2020	CMT	ER4043	-	Simulation – Interlayer temperature prediction	Utilise a finite element model to achieve continuous deposition while maintaining dimensional accuracy.	[47]
2020	CMT	Cu-8Al-2Ni-2Fe-2Mn alloy	100 °C - 400 °C	Effect interpass with ultrasonic vibration	Investigate the effect of varying the interpass temperature on the product characteristics with and without ultrasonic vibration.	[48]
2021	PAW	Ti6Al4V	500 °C	Effect of interpass	Examine the microstructure and mechanical properties of a novel twin wire plasma arc-based AM process.	[6]
2020	GMAW	ER70S-6	250 °C	Different idle time and Implemented air jet impingement	Air-jet impingement on deposited material was used to boost convective heat transfer rate.	[46]
2021	GMAW	ER420	25 °C and 200 °C	Effect of interpass temperature	Study the effect of resultant thermal history with different interpass temperatures applied and investigate the in-situ heat treatment.	[21]
2021	GTAW	AZ80M Mg alloy	150 °C		Examine the WAAM process heating cycle, microstructural evolution, and mechanical characteristics.	[20]
2021	GMAW	ER420	25 °C to 200 °C		Study effect of interlayer temperature and the correlation between interlayer temperature, microstructure, and corrosion properties.	[49]
2022	CMT	unalloyed steel G4Si1 (1.5130)	200 °C		Effect of interpass temperature, energy input and cooling rate on microsections, tensile test and Charpy v specimen.	[50]
2021	Pulsed GMAW	Stainless steel	160 °C + Cyogenic cooling	Improvement- Cryogenic cooling	Applied the process of cryogenic cooling and study the impact on developing microstructure and related mechanical properties	[51]

Table 1. (Continous) Primary studies

Year	Process	Material	Interpass	Key area	Aim of the study	Refs.
2021	GTAW	Fe_3Ni	200 °C	Implement in-situ neutron diffraction	Study the interpass and implement in-situ neutron diffraction	[52]
2023	CMT	WAAM wire	100 °C to 300 °C	Effect of heat control	Correlation of welding parameters and AM geometry based on resulting microstructure	[53]
2023	CMT	Nitinol wire with Ni50.9Ti49.1	200 °C and 400 °C	Optimize interlayer temperature	Study impact optimal interlayer temperature on porosity level, morphology, and mechanical characteristics	[34]
2024	GMAW	SDSS 2507	30 °C, 150 °C and 250 °C	Effect of interpass temperature	Determine effect on austenite ferrite ratio of WAAM structure	[54]
2024	CMT	Inconel 625	100 °C, 200 °C, 400 °C, and 600 °C		Influence of interpass temperature on microstructure and mechanical properties	[33]
2025		Inconel 625	150 °C and 350 °C		Optimization strategy to improve surface quality	[55]
2025	CMT	ER120S-G	100 °C and 300 °C		Correlation of thermal cycle process on microstructural changes.	[56]
2025	CMT	AWS ERTi-5	120 °C and 400 °C	Controlling interpass temperature	Monitoring effect of interpass temperature on mechanical properties and geometrical uniformity.	[57]
2025	CMT	Inconel 625	150 °C, 250 °C, and 350 °C	Effect of interlayer dwell time and interlayer temperature	To evaluate the change in geometric and mechanical properties	[33]

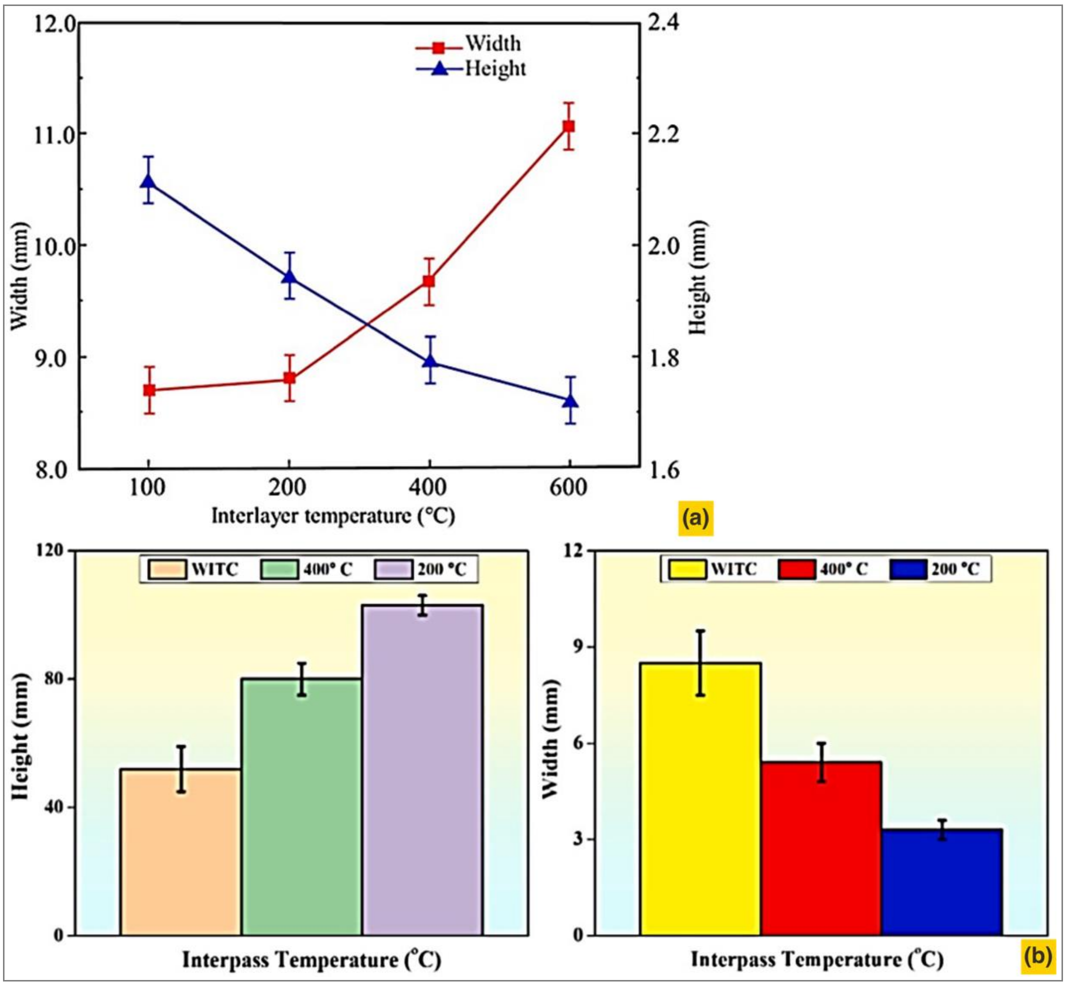

Figure 4. Effect of interpass temperature on height and width: (a) Temperature 100 °C to 600 °C [33]; (b) Without interlayer temperature control (WITC), 200 °C and 400 °C [34]

The narrow bead width in the first few layers was due to the rapid cooling of the molten pool to the calm substrate [22], [32]. The low amount of heat accumulated at the initial stage of the process calmed the substrate and acted as a heat sink allowing the heat flux to dissipate downward during the solidification process and generated a high-temperature gradient [48], [58]. The shape metal deposition process began when the substrate was preheated started. The deposit stabilised with additional post-heating until the steady-state molten pool achieved a stable temperature. Wu *et al*. investigated the impact of heat accumulation, interlayer surface oxidation, bead geometries, and metal transfer behaviour, particularly at the beginning of the build-up of the layers [18]. As the layer height rose owing to heat accumulation, the interpass temperature also increased. The subsequent layers will become contaminated if the interpass temperature was not adequately controlled. Therefore, in order to prevent further contamination, it is important to ensure an adequately low level of surface oxidation on the recently deposited layer.

Geng *et al*. used a theoretical model combined with Rosenthal's analytical solution to determine an optimum interpass temperature for each layer deposition [35]. The temperature of the interpass was gradually increased from room temperature to 25 °C, 50 °C, 80 °C, and 120 °C, improving the surface appearance progressively. As the interpass temperature increased, the premature solidifying process became slow resulting in an improved wettability of the molten metal. However, the initial preheating between 50 °C and 80 °C was insufficient to observe the undulated layer appearance. When the interpass temperature was increased to 120°C, the surface layer became smoother. Thus, exceeding this temperature is not recommended due to uneven layer cross-sectional dimensions.

Shen *et al*. [52] kept the interpass temperature constant at 200 °C throughout their fabrication process and discovered an enormous hot cracking defect in the bulk sample. Hence, neutrons were used to produce thermal phase evolution characteristics to prevent hot cracking during manufacturing. Wu *et al*. [31] added forced interpass cooling using compressed CO_2 into the deposition process to manage the deposition accuracy with interpass temperature application. The finding showed that forced interpass cooling expedited the construction process and maintained the deposition accuracy. Ogino *et al*. [37] suggested an alternative approach relying on numerical methods to readily forecast and regulate the WAAM process. According to the findings, the interpass temperature affected the deposition shape. Therefore, adjusting the temperature will result in a higher and faster deposition rate. This outcome demonstrated a consistency between the numerical and the experimental results.

In summary, regulating the different cooling rates throughout the deposition process is crucial in controlling the geometrical accuracy. Decreased interpass temperature shows the uniformity of the deposited wall bead and layer height. However, a decrease in the interpass temperature results in an asymmetrical deposition at the substrate due to an insufficient large weld pool to melt two different materials. Thus, it is necessary to increase the interpass temperature at a particular initial layer and to maintain this temperature to ensure equal heat dissipation with heat input. Additionally, using a cooling system is recommended to reduce the build time while retaining deposition accuracy.

5. Effect on Microstructure Behaviour and Mechanical Properties

The heat cycle of the material during production has a significant impact on the sample microstructure. The high-temperature gradient and multiple heating and cooling lead to additional microstructural variation. The variance is influenced by the number of thermal cycles of deposited layer endures during the manufacturing process. The proper microstructure is achieved by critically managing the cooling rate during welding. Idle time is the most used approach for reducing heat accumulation. However, extending the cooling time of the interlayer does not influence the accumulation occurrence and instead decreases the efficiency of part formation [65]. Attaining a homogeneous microstructure in additively manufactured parts is essential to achieving isotropic properties. Literature findings have shown that regulating the interlayer temperature affect grain development and geometry during deposition producing a homogeneous microstructure of WAAM parts.

The interpass temperature performed by previous researchers varied from the lowest at 25 °C [49], [59], 50 °C [35], [39], [44], 80 °C [30], [35], 100 °C [39], [48], and 120-125 °C [28], [30], [35], 150-160 °C [20], [35], [38], [39], [42], [51], 200-250 °C to the highest at 300-500 °C [6], [32], [42], [48]. Despite the different interpass and heat cycles, the microstructure can be divided into three distinct regions: the top, middle, and bottom regions close to the substrate. The cross-section of the as-build samples using the optical microscopy revealed the microstructural characteristic. Additionally, the grain structure is also critical because it affects the mechanical properties of an alloy.

5.1. Titanium alloy, Ti-6Al-4v

The interpass temperature significantly influences the intricate microstructure and resulting mechanical properties of Ti-6Al-4V components fabricated via Wire Arc Additive Manufacturing. Controlling the cooling rate through interpass temperature is crucial for managing the formation of different phases (α, α′, β) and grain characteristics, which directly impacts the material's strength and ductility.

The microstructure and mechanical properties of Ti-6Al-4V wire material using various heat source-based WAAM processes are summarised in **Table 2**. The temperature measured during the interpass is also included for comparison. Several researchers investigated the effect of interpass on Ti-6Al-4V material microstructure prepared using PAW, GMAW, and GTAW-based AM process [6], [18], [29], [43], [57]. The results showed that the microstructure of Ti-6Al-4V was different in two regions of the α and β phases and was characterised by the size described as fine or coarse and the arrangement as lamellar or equiaxed. According to Wu *et al*. [31] near-equiaxed beta β grains was formed in the substrate region, lamellar α interwoven with a course Windmanstatten structure was formed in the intermediate area and acicular α' incorporated with a basketweave structure was formed at the top as shown in **Figure 5**. Therefore, it was well established that deposited Ti-6Al-4V consisted primarily of α', α, and β phases, and only the α' phase was formed at high cooling rates on the top region. When the interpass temperature was increased to 300 °C, a similar microstructure was observed, with the grain being noticeably more prominent. Thus, this finding demonstrated the microstructure is uniform due to grain growth at a slow cooling rate.

When CO_2 is added, the amount of lamellar α is replaced, allowing the interwoven structure of the acicular α' grain to be more clearly visible [31]. In their study, Wu *et al*. [29] recommended that the interpass temperature be kept below 200 °C to retain an acceptable condition of fabricated Ti-6Al-4V. The microstructure revealed a large colony α formed at the top layers that enriched the previous β grain and grain boundary α phase. The microstructure also showed that the grain structure was enhanced from bottom to middle.

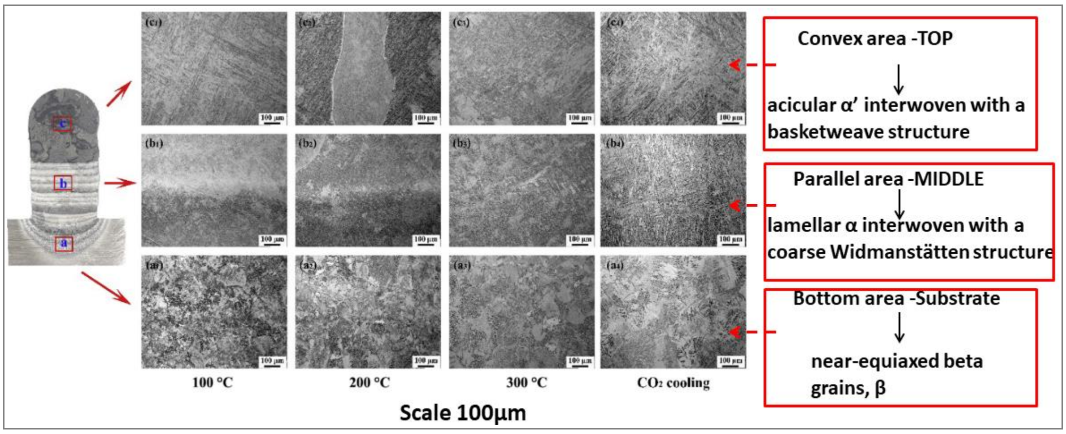

Figure 5. The microstructures of parts fabricated under different process conditions adapted from studies by Wu *et al*. [63]

Yi *et al*. [43] demonstrated that samples manufactured without water cooling produced coarse grain structures. In contrast, models manufactured with water cooling by controlling the interpass temperature at 15°C created a more delicate grain structure. As a result, the α phase was formed along the prior β grain boundary in all areas while the WAAM Ti–6Al–4V alloys formed complexly shaped Widmanstätten structure (α + α′ phase) inside these areas. Additionally, with rapid cooling and fine-grain formation, the cold specimen had higher Vickers hardness and tensile strength than the original specimen. Wang *et al*. [6] reported a similar microstructure trend with a lamellar colony in the middle region and a dendritic grain with equiaxed grain in the top area at 500 °C interpass temperature.

Rapid cooling and phase transformations that vary from equilibrium are two characteristics of the process. Moreover, the tensile properties are comparable to the base metal value ranging between 958 MPa and 1049 MPa. However, when the interpass temperature exceeds 200 °C, the mechanical properties are considerably compromised. The production of more acicular α reduces in the interstitial content and α lamellar boundary spacing lowers the mechanical strength. The higher the interpass temperature will increase oxide content, which could lead to decreased mechanical properties such as embrittlement to structural alloys [44].

Further, the study was focused on increasing lamellar and acicular structure of grains and the effect of grain structure on mechanical properties. Generally, as the number of layers increases, the number of grains decreases as the size increases. There are no appreciable changes in the microstructure as interpass temperature changes. The structure is still the same but varied in the size, either refined or coarse, depending on the interpass temperature difference. However, with the inclusion of the cooling system, the interpass temperature is lowered, resulting in a more delicate grain structure and increased strength.

Table 2. Summaries of Ti-6Al-4V, microstructure and mechanical properties

Process	Interpass Temperature	Microstructure	UTS	Notes	Refs.
PAW	500 °C	Fully lamellar colony in the middle; and equiaxed dendritic at top.	-	Severe coarsening and lower strength	[6]
GMAW	15 °C (Cooling water)	Origin – Coarse Widmanstätten structure (α + α′ phase) Cold - Fine Widmanstätten structure (α + α′ phase)	The strength and hardness of the original specimen are lower than the strength and hardness of the cold specimen	High hardness, improved ductility	[43]
GTAW	100 °C, 200 °C, 300 °C, and gas cooling	Bottom - Beta grain, β Middle – Lamellar α interwoven with coarse Widmanstätten Top - Acicular α' interwoven with basketweave structures	897±50 MPa, 852±52 MPa, 847±35 MPa, and 913±17 MPa.	Microstructure evolution and hardness not greatly affected by interpass temperature, however it affects geometric accuracy of deposited layer	[31]
GTAW	200 °C	Lathlike matrix structure at bottom, lamellar α and basketwave structures in middle; and colony α structure at top	958 MPa - 1049 MPa	Recommended <200°C to avoid excessive coarsening	[29]
CMT	120 °C and 400 °C	The higher the interpass temperature, the large the grain size. Microstructures compose α′ martensite and similar between the layers.	950 MPa – 975 MPa	Higher temperature, higher strength but lower ductility	[57]

5.2. Stainless Steel

Knezovic *et al*. [39] and A Hosseini *et al*. [38] deposited duplex stainless steel (DSS) using a GMAW-based WAAM process to investigate the effect of the interpass temperature on the structure and properties of the produced material. According to Knezonic *et al*. [39], controlling interpass while depositing DSS with the WAAM process reduced the excessive ferrite amount, which was a typical problem in DSS. Knezonic *et al*. [39] found when increasing the interlayer temperature to 150 °C it help to reduce the ferrite content. Furthermore, the amount of ferrite was more significant at lower interlayer temperature due to the transition to ferrite that occurred while the layer cooled and insufficient heat input to cause the transformation to austenite. Besides, resulting in higher hardness and strength at 150 °C of interpass temperature [54]. Thus, the higher interlayer temperature was preferred because it allowed for faster parts production while maintaining a fine ferrite. A Hosseini *et al*. [38] compared the results produced with a low interlayer temperature and a low heat input sample with a high interlayer temperature and a high heat input sample. Similar to Knezonic *et al*. [39], a more significant ferrite fraction was observed at low interlayer temperatures and less heat input. In summary, as the layer deposited increased, primary austenite grew and secondary austenite formed between primary austenite grains [38].

Although the stainless-steel types vary, Salahi *et al*. [49] and Nameni *et al*. [39] discovered that the retained austenite phase increases as the interpass temperature increases from 25 °C to 250 °C. **Table 3** presents a summary of the influence of interpass temperature on stainless steel components. This observation indicated that to achieve the ideal microstructure, a high interlayer temperature must be properly controlled. It is also preferable to add an acceptable amount of ferrite to improve the speed of the part production faster. According to Prathivraj *et al*. [54] the austenite-ferrite ratio is greatly enhanced at 150 °C because of low cooling rate and promotes the formation of austenite. Stainless steel does not harden by heat treatment, and no austenite transformation to martensite occurs during cooling. Thus, the absence of martensite eliminates the need for preheating and controlling the minimum interpass temperature and there is no risk of cold cracking. Therefore, to retain the corrosion resistance of the stainless steel, the maximum interpass temperature should be maintained and not exceed 150 °C.

Table 3. Summaries of stainless-steel components microstructure and mechanical properties

Process	Material	Interpass temperature	Microstructure	Refs.
Pulsed-GMAW	Stainless steel 316L	160 °C+Cyogenic cooling	Large columnar grains aligned to the build direction	[51]
GMAW	Duplex stainless steel (DSS)	50 °C, 100 °C and 150 °C	More ferrite is produced with lower interlayer temperature. Low ferrite amount at high interlayer and significantly reduces porosity. Ferrite amount and porosity, it is strongly suggested to use higher interlayer temperatures	[39]
GMAW	Duplex stainless steel (DSS)	150 °C and 250 °C	Ferritic matrix with mostly grain boundary and Widmanstätten austenite	[38]
GMAW	ER420, SS	25 °C to 200 °C	200 °C- Anisotropic crystallographic behaviour 25 °C – Isotropic texture 25 °C to 200 °C – Phase retained austenite	[49]
GMAW	ER420, SS	25 °C and 200 °C	25 °C – Interdendritic delta ferrite phase embedded in a martensitic matric with a negligible amount of retained austenite 200 °C – A higher fraction of retained austenite was stabilised in the martensite lathes	[21]
GMAW	Duplex Stainless Steel (DSS)	30 °C, 150 °C, and 250 °C	Austenite-ferrite ratio at 150 °C interpass temperature resulting higher hardness and strength	[54]

5.3. Aluminium Alloy and Steel

Numerous researchers have developed an aluminium alloy using the WAAM technique [28], [30], [41], [44], [45]. Due to its wide range of applications, aluminium (Al) is one of the most experimented with metals in the WAAM process. Al alloys are gaining increased attention due to their relatively low density and widespread use in aviation, aerospace, and automotive [60]. However, welding an Al alloy has proven difficult to create an aluminium oxide layer due to its porosity and solidification behaviour [61], [62]. Therefore, reducing porosity is a crucial concern in manufacturing Al using the WAAM process [63].

Furthermore, not all Al alloys are heat treatable, which constrained the evaluation of the influence of heat treatment on the Al WAAM process component. **Table 4** summarises the studies by some researchers who explored the effect of interpass temperature variation on the porosity content and mechanical properties of the WAAM process. Moreover, comprehensive review of numerous significant findings to reveal that increasing the interpass temperature will result in a decrease in the porosity of samples fabricated using the pulse GMAW method [44], [45]. When compared with a sample made using the CMT-based WAAM process, the result showed that the influence of interpass temperature on porosity number had reversed [44]. Ren *et al*. [30] also discovered a similar result when conducting an experiment with the CMT-WAAM process where the diameter of the pores decreased to <100 µm with interpass temperatures increase. Adjusting the dwell time produced a similar trend when using pulse-MIG and CMT. Furthermore, when the Al-5356 solid wire was deposited using CMT-pulse mode with a longer dwell time, more fine porosity was discovered [28]. Therefore, reducing the interpass temperature significantly refines the grain, minimising undesirable elements deposition and microstructure homogeneity. Studies showed that porosity occurs primarily due to the hydrogen content [64], [65]. Pulse GMAW has a higher pore content than CMT because it picks up more hydrogen than CMT. Due to increased interpass temperature, pulse GMAW is able to maintain a lower percentage of absorbed hydrogen in solid solution than CMT. During the solidification phase, the remaining hydrogen is used in pore formation. Wang *et al*. [66] stated that CMT is more susceptible to porosity generation when compared to GMAW due to its lower transition temperature and a shorter gas escape time. Lowering the interpass temperature could significantly improve the mechanical properties. When comparing the results of the sample produced at 200 °C and 80 °C interpass temperature, the horizontal elongation increased by 12%, while the vertical tensile strength, YS and the elongation improved by 25%, 36%, and 113%, respectively [30]. In contrast to the sample produced with GMAW, the strength reduced when interpass temperature was lowered due to the increased in pore number. However, the horizontal direction sample showed better tensile strength than the vertical sample [45].

Table 4. Brief description of Aluminium alloy component fabricated by WAAM process

Process	Material	Interpass	Microstructure	Refs.
CMT-ADV	Al-6.3Mg alloy	200 °C, 160 °C, 120 °C, and 80 °C	• 160 °C – 200 °C: Layer and interlayer easily recognised. Grains sizes are acceptable, 30 -50 µm. Equiaxed crystal • 80 °C – 120 °C: Dendrite eliminated, and fine equiaxed crystal is no significant difference between layer and interlayer. • The number of pores decreased; they were all <50 µm	[30]
Pulse CMT	Al-5356	Time: 30/60/120 T<60, Temp 125 °C	• Near fusion line – Fine grains microstructure and high microhardness formed. • The region below interlayer – Coarse grain microstructure with an increased formation of segregations • Interlayer zone – Further increased occurrence of segregation is identified.	[28]
Pulse GMAW, CMT	ER5183	50 °C and 100 °C Interlayer dwell time 30 and 120s	• The number of pores increases when deposited using Pulse GMAW than CMT. • Low interlayer temperature for pulse GMAW shows porosity content increase compared to the high interlayer. However, the reverse result for CMT	[44]
Pulsed-GMAW	Al-5356	50 °C and 100 °C 50 °C – 0.02035 % porosity 100 °C - 0.01823% porosity	• 50 °C – 0.02035 % porosity 100 °C - 0.01823% porosity • Pore volume - 0.01 to 0.05 mm³ contributed 85% of total pore in both interpass. - 0.05 to -0.15 mm³ counted 14% more in higher interpass than low interpass. • The low interpass showed more grain than the higher interpass sample.	[45]

5.4. Other Metals

The impact of Interpass temperature using the WAAM technique has been studied on other metals as well, such as mild steel, H3Si1 [40], Fe3Ni-FeNi compositionally graded material (FGM) [52], AZ80M Magnesium (Mg) alloy [20], Fe3Al-based iron aluminide [32], ISO 14341-A-G 50 7 M21 4Mo [42] and ER110S – Mild steel [22]. **Table 5** summarises the effect of interpass temperature on the microstructure and mechanical properties of several materials manufactured using the WAAM process. Most of these studies were focused on identifying the significant importance of WAAM interpass temperature control. The microstructure and mechanical properties of as-built components were studied and correlated with the thermal cycle in the WAAM process. Generally, the results showed a slightly elongated crystal grains were observes at the bottom, a more refined grain was visible in the middle, and a more prominent grain was seen in the heat sink direction. When the interpass temperature was set at a constant, the columnar grain grew and remained stable along the build direction. Therefore, the interpass temperature of 150 °C is recommended for fabricating the WAAM process, and as the interlayer temperature increases, the yield strength decreases. According to Shen *et al*. [52], increasing the interpass temperature has little effect on the WAAM process, but expanding the deposition current could cause the columnar grain to continue growing.

Table 5. Microstructure and mechanical properties of various WAAM processes

Process	Material	Interpass	Microstructure	YS (MPa)	UTS (MPa)	EL (%)	Refs.
GMAW	Mid steel filler wire, H3Si1 1.2 mm.	Comparing three methods, Interpass selected = 150 °C	Bottom: Slightly elongated crystal Middle: Fine grain Top: larger grain visible and grow in the direction of a heat sink	The tensile test for all three specimens shows no difference in the microstructure. Forced air cooling along the deposition path improved productivity by up to 30% compared with the deposition without cooling.			[40]
GTAW	Functionally graded material (FGM)	200 °C	Large columnar grains grow along the build-up direction	-	[52]	-	[51]
GTAW	AZ80M Mg alloy	150 °C	Bottom – Epitaxial growth Middle–Dendrite segregation but less than a top Top – Reveal the number equiaxed and dendritic	V - 119±13.4 H - 146±14.7	[20]	V - 7±0.2 H- 15±0.5	[23]
GTAW	Fe3Al-based iron aluminide	400 °C	Increasing deposition current – columnar grains larger and interpass not markedly influence - size columnar grains in the bottom section are much smaller then in the middle.	847.7 ± 2.5	[32]	3.3 ± 0.1	[53]
		360 °C		844.8 ± 25.7	945.2 ± 26.4	3.3 ± 0.2	
		320 °C		705.9 ± 31.7	827.1 ± 30.5	3.1 ± 0.6	
		280 °C		642.8 ± 34.3	764.5 ± 22.8	2.8 ± 0.3	
GMAW	ISO 14341-A-G 50 7 M21 4Mo	150 °C and 300 °C	- The microstructure is essentially homogeneously distributed for both interlayer temperatures. - Microstructure consists mainly of globular ferrite and pearlite for both interlayer temperatures.	The yield strength decreases slightly when the interlayer temperature is increased.			[42]
GMAW	ER110S – Mild steel	800 to 500 °C	At higher temp leading the formation of the coarse grain HAZ or recrystallisation forming fine grain HAZ	-	-	-	[22]

6. Current Methods for Quality Improvement in the WAAM Process

In addition to controlling the interpass temperature, several researchers attempted to improve the process to control the microstructural evolution, as shown in **Figure 6**. Cunningham *et al*. [51] proposed fabricating with Pulse GMAW and applying a cryogenic cooling system. The results showed that the interpass temperature contained larger columnar grains aligned to the build direction. The sample produced contained grains that were reduced in size and texture with a feather morphology. In addition, the tensile strength also increased during the cooling process. Hackenhaar *et al*. [46] proposed air jet impingement with interlayer idle time from 30 seconds to 120 seconds. The result indicated that when air jet impingement was used, the substrate temperature did not further reduce, and the idle time rose from 30 seconds to 120 seconds. However, despite the 10 seconds of idle time and the application of air-jet impingement, an increase in substrate temperature was significantly reduced [46]. Another cooling method was developed by Wang *et al*. using the WAAM technique in combination with a novel online vortex cooling system. This online cooling source was able to reduce common flaws such as low forming precision, coarse grains, and pores produced by heat accumulation in the WAAM process [41]. Some researchers proposed using simulation and modelling to improve the WAAM heat accumulation. Montevecchi *et al*. [36] presented a novel approach for the WAAM process by scheduling the interlayer idle intervals during deposition. The result obtained was verified by comparing the measured temperature to the FE simulation result. The FE simulation accurately determined the WAAM workpiece thermal behaviour, and the adoption of idle intervals had prevented severe structural collapses. Also, it maintained a consistent interpass temperature and a constant molten pool size.

Ogino *et al*. [37] investigated the deposition procedure numerically on the deposition shape and carried out experimentsto verify the results. The CMT based WAAM was conducted to deposit mild steel welding wire with low heat input. The results differed between simulation and experiment, and a similar tendency was found depending on the condition. Consequently, the deposition form was determined by the interpass temperature and was appropriately set to achieve a more significant and thinner deposition. Other simulations were recommended to fabricate a WAAM technique specification using the developed model and to validate the effect by manufacturing the wall part [35].

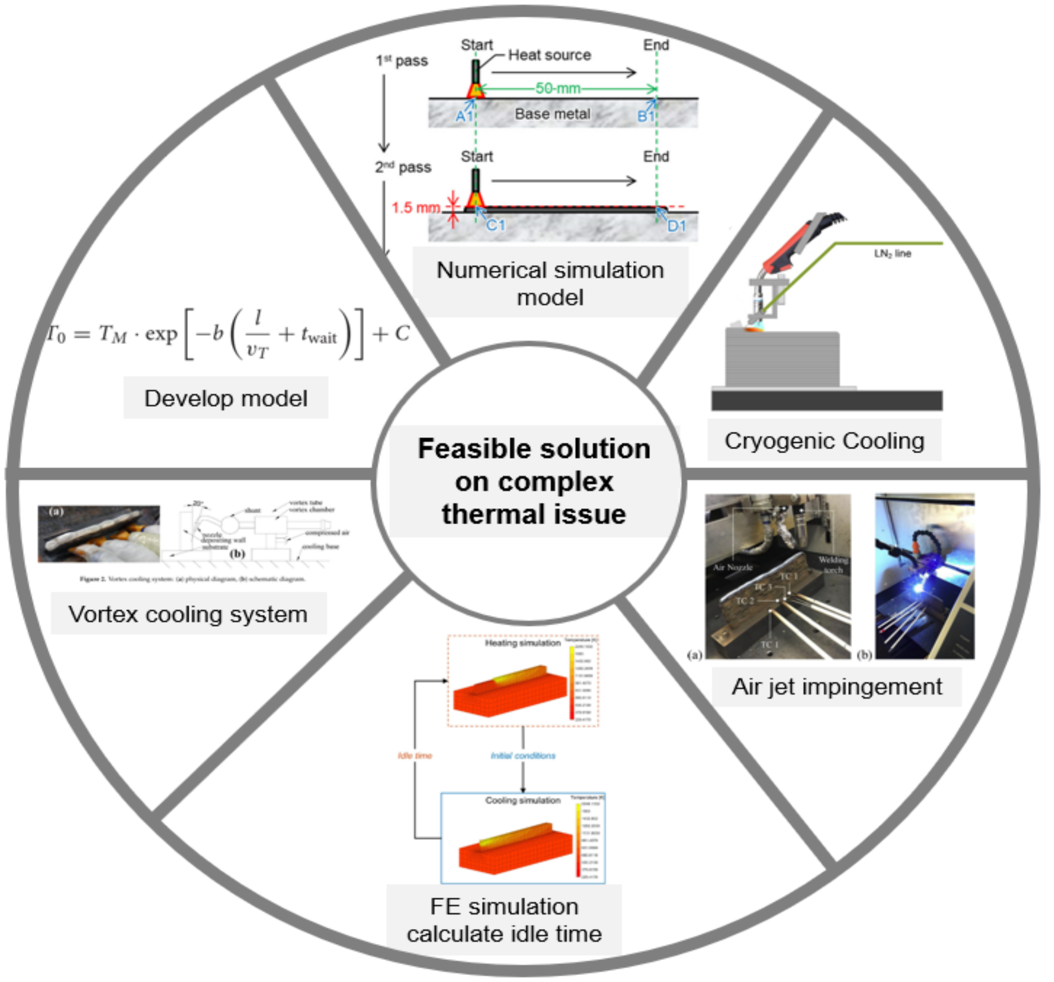

Figure 6. Overview of feasible solutions to improve heat accumulation in the WAAM process

7. Conclusion and Recommendation

In this review, the effect of interpass temperature on the surface morphologies, microstructure, and mechanical properties has been systematically review. The finding include:

- Interpass temperature significantly influences surface morphologies, where higher interpass temperature generally produce wider and flatter weld bead. The optimum interpass temperature in the range of 120 – 200 °C is recommended to enhance smooth surface and geometric stability.
- The interpass temperatures below 200 °C for Ti-6Al-4V are critical to refine microstructure and increase strength, as higher temperatures leads to grain coarsening and reduce mechanical performance.
- In WAAM stainless steel, the balance ratio of ferrite and austenite content is greatly enhanced at 150 °C thereby increase hardness and strength.

Although a higher interpass temperature may reduce the tendency to produce coarse grain, it is not specified for high-strength steel. The results for samples obtained using pulse GMAW and CMT-based WAAM processes showed the presence of hydrogen in aluminium material deposit to be reversed. Hence, the mechanical properties can significantly be enhanced by lowering the interpass temperature. However, pulse GMAW-based WAAM produces a different result because it picks up more hydrogen when interpass temperature is low and produces higher pore content.

Therefore, the challenge is to maintain the interpass temperature to above minimum between passes in order to reduce or eliminate the risk of cold weld cracking. Based on the review of all related papers, the maximum interpass temperature of 150 °C is recommended. Thus, interpass temperature can have both minimum and maximum values depending on the deposited material. The recommendation includes using a cooling system such as CO_2 and water to help speed up the cooling deposition and deposition shape to achieve an excellent and thinner deposition. Water cooling produces delicate grain structures by controlling the interpass temperature of Ti-6Al-4v. Moreover, heat accumulation can be minimised by ensuring equal heat input and dissipation. Effective interpass temperature control is not merely an academic pursuit but holds significant implications for industrial applications. By ensuring optimal material properties and dimensional accuracy, it can lead to reduced post-processing, decreased material waste, and improved energy efficiency, thereby contributing to more sustainable and cost-effective manufacturing practices in sectors such as aerospace, automotive, and construction. Thus, to produce components with high quality and accuracy, it is essential to investigate the effects of interpass temperature in the WAAM manufacturing process.

Acknowledgements

The study is funded by Ministry of Higher Education (MOHE) of Malaysia, through the Fundamental Research Grant Scheme (FRGS), No: FRGS/1/2024/TK10/UTEM/03/3, FRGS-EC/1/2024/FTKIP/F00599.The authors also would like to thank you Universiti Teknikal Malaysia Melaka (UTeM) for all the supports.

Authors’ Declaration

Authors’ contributions and responsibilities - All authors contributed to the conception and development of the review. The authors contributed to the literature search, analysis and synthesis of the relevant studies, discussion of the findings, and preparation and revision of the manuscript. All authors reviewed and approved the final version of the manuscript.

Funding – This research was funded by Ministry of Higher Education (MOHE) of Malaysia, through the Fundamental Research Grant Scheme (FRGS), No: FRGS/1/2024/TK10/UTEM/03/3, FRGS-EC/1/2024/FTKIP/F00599.

Availability of data and materials - The data and information reviewed in this study were obtained from publicly available published literature. All relevant sources are cited within the manuscript.

Competing interests - The authors declare no competing interests.

Generative AI statement - During the preparation of this manuscript, the authors used generative artificial intelligence tools for language editing and proofreading purposes only. The authors reviewed and edited the content and take full responsibility for the content of the published manuscript.

Additional information – No additional information from the author.

References

[1] M. Srivastava, S. Rathee, A. Tiwari, and M. Dongre, “Wire arc additive manufacturing of metals: A review on processes, materials and their behaviour,” *Materials Chemistry and Physics*, vol. 294, no. May 2022, p. 126988, 2023, doi: 10.1016/j.matchemphys.2022.126988.

[2] J. González, I. Rodríguez, J. L. Diéguez, and A. Pereira, “Additive manufacturing with GMAW welding and CMT technology,” *Procedia Manufacturing*, vol. 13, no. December, pp. 840–847, 2017, doi: 10.1016/j.promfg.2017.09.189.

[3] J. EL Mesbahi, I. Buj-Corral, and A. EL Mesbahi, “Use of the QFD method to redesign a new

extrusion system for a printing machine for ceramics," *The International Journal of Advanced Manufacturing Technology*, vol. 111, no. 1–2, pp. 227–242, Nov. 2020, doi: 10.1007/s00170-020-05874-x.

[4] C. M. González-Henríquez, M. A. Sarabia-Vallejos, and J. Rodriguez-Hernandez, "Polymers for additive manufacturing and 4D-printing: Materials, methodologies, and biomedical applications," *Progress in Polymer Science*, vol. 94, pp. 57–116, Jul. 2019, doi: 10.1016/j.progpolymsci.2019.03.001.

[5] Z. Y. Chua, I. H. Ahn, and S. K. Moon, "Process monitoring and inspection systems in metal additive manufacturing: Status and applications," *International Journal of Precision Engineering and Manufacturing-Green Technology*, vol. 4, no. 2, pp. 235–245, Apr. 2017, doi: 10.1007/s40684-017-0029-7.

[6] L. Wang *et al.*, "Twin-wire plasma arc additive manufacturing of the Ti–45Al titanium aluminide: Processing, microstructures and mechanical properties," *Intermetallics*, vol. 136, no. March, p. 107277, Sep. 2021, doi: 10.1016/j.intermet.2021.107277.

[7] F. Ciccone, A. Bacciaglia, and A. Ceruti, "Optimization with artificial intelligence in additive manufacturing: a systematic review," *Journal of the Brazilian Society of Mechanical Sciences and Engineering*, vol. 45, no. 6, p. 303, Jun. 2023, doi: 10.1007/s40430-023-04200-2.

[8] X. Zhang, L. Chen, T. Mulholland, and T. A. Osswald, "Effects of raster angle on the mechanical properties of PLA and Al/PLA composite part produced by fused deposition modeling," *Polymers for Advanced Technologies*, vol. 30, no. 8, pp. 2122–2135, Aug. 2019, doi: 10.1002/pat.4645.

[9] C. Dharmendra, B. S. Amirkhiz, A. Lloyd, G. D. J. Ram, and M. Mohammadi, "Wire-arc additive manufactured nickel aluminum bronze with enhanced mechanical properties using heat treatments cycles," *Additive Manufacturing*, vol. 36, no. August, p. 101510, 2020, doi: 10.1016/j.addma.2020.101510.

[10] F. A. Cruz Sanchez, H. Boudaoud, M. Camargo, and J. M. Pearce, "Plastic recycling in additive manufacturing: A systematic literature review and opportunities for the circular economy," *Journal of Cleaner Production*, vol. 264, p. 121602, Aug. 2020, doi: 10.1016/j.jclepro.2020.121602.

[11] ASTM International, "Additive Manufacturing - General Principles Terminology (ASTM52900)," 2013. doi: 10.1520/F2792-12A.2.

[12] D. Sarathchandra and M. Davidson, "Effect of heat input on mechanical and microstructural properties of Inconel 625 depositions processed in wire arc additive manufacturing," *Proceedings of the Institution of Mechanical Engineers, Part E: Journal of Process Mechanical Engineering*, vol. 235, no. 5, pp. 1439–1448, Oct. 2021, doi: 10.1177/09544089211004718.

[13] D. W. Rathod, "A Review on challenges and opportunities in wire arc additive manufacturing of aluminium alloys: Specific context of 7xxx series alloys," *Mechanical Engineering for Society and Industry*, vol. 5, no. 1, pp. 107–124, Mar. 2025, doi: 10.31603/mesi.12711.

[14] K. Treutler and V. Wesling, "The current state of research of wire arc additive manufacturing (Waam): A review," *Applied Sciences (Switzerland)*, vol. 11, no. 18, 2021, doi: 10.3390/app11188619.

[15] P. S. Kumar, L. S. Raju, and L. S. R. Krishna, *A Review on Wire Arc Additive Manufacturing (WAAM) Fabricated Components of Ti6AL4V and Steels*, vol. 1, no. i. Springer International Publishing, 2020. doi: 10.1007/978-3-030-24314-2.

[16] E. Aldalur, F. Veiga, A. Suárez, J. Bilbao, and A. Lamikiz, "High deposition wire arc additive manufacturing of mild steel: Strategies and heat input effect on microstructure and mechanical properties," *Journal of Manufacturing Processes*, 2020, doi: 10.1016/j.jmapro.2020.08.060.

[17] A. Queguineur, G. Rückert, F. Cortial, and J. Y. Hascoët, "Evaluation of wire arc additive manufacturing for large-sized components in naval applications," *Welding in the World*, vol. 62, no. 2, pp. 259–266, Mar. 2018, doi: 10.1007/s40194-017-0536-8.

[18] B. Wu *et al.*, "Effects of heat accumulation on the arc characteristics and metal transfer behavior in Wire Arc Additive Manufacturing of Ti6Al4V," *Journal of Materials Processing Technology*, vol. 250, pp. 304–312, 2017, doi: 10.1016/j.jmatprotec.2017.07.037.

[19] A. Jaisingh Sheoran and H. Kumar, "Fused Deposition modeling process parameters

optimization and effect on mechanical properties and part quality: Review and reflection on present research," *Materials Today: Proceedings*, vol. 21, pp. 1659–1672, 2020, doi: 10.1016/j.matpr.2019.11.296.

[20] Y. Guo, G. Quan, Y. Jiang, L. Ren, L. Fan, and H. Pan, "Formability, microstructure evolution and mechanical properties of wire arc additively manufactured AZ80M magnesium alloy using gas tungsten arc welding," *Journal of Magnesium and Alloys*, vol. 9, no. 1, pp. 192–201, Jan. 2021, doi: 10.1016/j.jma.2020.01.003.

[21] A. Vahedi Nemani, M. Ghaffari, S. Salahi, J. Lunde, and A. Nasiri, "Effect of interpass temperature on the formation of retained austenite in a wire arc additive manufactured ER420 martensitic stainless steel," *Materials Chemistry and Physics*, vol. 266, no. January, p. 124555, Jul. 2021, doi: 10.1016/j.matchemphys.2021.124555.

[22] T. A. Rodrigues, V. Duarte, J. A. Avila, T. G. Santos, R. M. Miranda, and J. P. Oliveira, "Wire and arc additive manufacturing of HSLA steel: Effect of thermal cycles on microstructure and mechanical properties," *Additive Manufacturing*, vol. 27, pp. 440–450, May 2019, doi: 10.1016/j.addma.2019.03.029.

[23] A. Scotti, "The Potential of IR Pyrometry for Monitoring Interpass Temperature in Wire + Arc Additive Manufacturing," *Evolutions in Mechanical Engineering*, vol. 3, no. 1, Sep. 2019, doi: 10.31031/EME.2019.03.000553.

[24] A WS Committee on Structural Welding, *Structural Welding Code - Steel.*, 17th ed., vol. 552, no. 20. United States of America, 1981.

[25] N. A. Rosli, M. R. Alkahari, M. F. bin Abdollah, S. Maidin, F. R. Ramli, and S. G. Herawan, "Review on effect of heat input for wire arc additive manufacturing process," *Journal of Materials Research and Technology*, vol. 11, pp. 2127–2145, Mar. 2021, doi: 10.1016/j.jmrt.2021.02.002.

[26] F. Martina, J. Ding, S. Williams, A. Caballero, G. Pardal, and L. Quintino, "Tandem metal inert gas process for high productivity wire arc additive manufacturing in stainless steel," *Additive Manufacturing*, vol. 25, no. November 2018, pp. 545–550, 2019, doi: 10.1016/j.addma.2018.11.022.

[27] X. Fang *et al.*, "Correlations between microstructure characteristics and mechanical properties in 5183 aluminium alloy fabricated by wire-arc additive manufacturing with different arc modes," *Materials*, vol. 11, no. 11, 2018, doi: 10.3390/ma11112075.

[28] M. Köhler, J. Hensel, and K. Dilger, "Effects of Thermal Cycling on Wire and Arc Additive Manufacturing of Al-5356 Components," *Metals*, vol. 10, no. 7, p. 952, Jul. 2020, doi: 10.3390/met10070952.

[29] B. Wu, Z. Pan, D. Ding, D. Cuiuri, and H. Li, "Effects of heat accumulation on microstructure and mechanical properties of Ti6Al4V alloy deposited by wire arc additive manufacturing," *Additive Manufacturing*, vol. 23, no. May 2017, pp. 151–160, Oct. 2018, doi: 10.1016/j.addma.2018.08.004.

[30] L. Ren *et al.*, "Effects of Interpass Cooling on Material Properties of Wire Arc Additive Manufactured Al–6.3Mg Alloy," *3D Printing and Additive Manufacturing*, vol. 6, no. 6, pp. 344–353, Dec. 2019, doi: 10.1089/3dp.2019.0061.

[31] B. Wu, Z. Pan, D. Ding, D. Cuiuri, H. Li, and Z. Fei, "The effects of forced interpass cooling on the material properties of wire arc additively manufactured Ti6Al4V alloy," *Journal of Materials Processing Technology*, vol. 258, no. October 2017, pp. 97–105, 2018, doi: 10.1016/j.jmatprotec.2018.03.024.

[32] C. Shen, Z. Pan, D. Cuiuri, D. Ding, and H. Li, "Influences of deposition current and interpass temperature to the Fe3Al-based iron aluminide fabricated using wire-arc additive manufacturing process," *The International Journal of Advanced Manufacturing Technology*, vol. 88, no. 5–8, pp. 2009–2018, Feb. 2017, doi: 10.1007/s00170-016-8935-3.

[33] D. Guo, T. Wang, J. Tang, M. Wang, and L. Li, "Influence of Interlayer Temperature on Microstructure and Mechanical Properties of Additively Manufactured Inconel 625," *Journal of Materials Engineering and Performance*, vol. 33, no. 22, pp. 12216–12226, 2024, doi: 10.1007/s11665-023-08875-5.

[34] S. Singh, I. A. Palani, S. Dehghani, C. P. Paul, K. G. Prashanth, and A. J. Qureshi, "Influence of the interlayer temperature on structure and properties of CMT wire arc additive manufactured NiTi structures," *Journal of Alloys and Compounds*, vol. 966, no. July, p. 171447,

Dec. 2023, doi: 10.1016/j.jallcom.2023.171447.

[35] H. Geng, J. Li, J. Xiong, and X. Lin, “Optimisation of interpass temperature and heat input for wire and arc additive manufacturing 5A06 aluminium alloy,” *Science and Technology of Welding and Joining*, vol. 22, no. 6, pp. 472–483, Aug. 2017, doi: 10.1080/13621718.2016.1259031.

[36] F. Montevecchi, G. Venturini, N. Grossi, A. Scippa, and G. Campatelli, “Idle time selection for wire-arc additive manufacturing: A finite element-based technique,” *Additive Manufacturing*, vol. 21, pp. 479–486, 2018, doi: 10.1016/j.addma.2018.01.007.

[37] Y. Ogino, S. Asai, and Y. Hirata, “Numerical simulation of WAAM process by a GMAW weld pool model,” *Welding in the World*, vol. 62, no. 2, pp. 393–401, Mar. 2018, doi: 10.1007/s40194-018-0556-z.

[38] V. A Hosseini, M. Högström, K. Hurtig, M. A. Valiente Bermejo, L. E. Stridh, and L. Karlsson, “Wire-arc additive manufacturing of a duplex stainless steel: thermal cycle analysis and microstructure characterization,” *Welding in the World*, vol. 63, no. 4, pp. 975–987, 2019, doi: 10.1007/s40194-019-00735-y.

[39] N. Knezović, I. Garašić, and I. Jurić, “Influence of the Interlayer Temperature on Structure and Properties of Wire and Arc Additive Manufactured Duplex Stainless Steel Product,” *Materials*, vol. 13, no. 24, p. 5795, Dec. 2020, doi: 10.3390/ma13245795.

[40] N. Kozamernik, D. Bračun, and D. Klobčar, “WAAM system with interpass temperature control and forced cooling for near-net-shape printing of small metal components,” *The International Journal of Advanced Manufacturing Technology*, vol. 110, no. 7–8, pp. 1955–1968, Sep. 2020, doi: 10.1007/s00170-020-05958-8.

[41] B. Wang, G. Yang, S. Zhou, C. Cui, and L. Qin, “Effects of On-Line Vortex Cooling on the Microstructure and Mechanical Properties of Wire Arc Additively Manufactured Al-Mg Alloy,” *Metals*, vol. 10, no. 8, p. 1004, Jul. 2020, doi: 10.3390/met10081004.

[42] M. Wächter *et al.*, “Monotonic and Fatigue Properties of Steel Material Manufactured by Wire Arc Additive Manufacturing,” *Applied Sciences*, vol. 10, no. 15, p. 5238, Jul. 2020, doi: 10.3390/app10155238.

[43] H.-J. Yi, J.-W. Kim, Y.-L. Kim, and S. Shin, “Effects of Cooling Rate on the Microstructure and Tensile Properties of Wire-Arc Additive Manufactured Ti–6Al–4V Alloy,” *Metals and Materials International*, vol. 26, no. 8, pp. 1235–1246, Aug. 2020, doi: 10.1007/s12540-019-00563-1.

[44] K. S. Derekar *et al.*, “Effect of pulsed metal inert gas (pulsed-MIG) and cold metal transfer (CMT) techniques on hydrogen dissolution in wire arc additive manufacturing (WAAM) of aluminium,” *International Journal of Advanced Manufacturing Technology*, vol. 107, no. 1–2, pp. 311–331, Mar. 2020, doi: 10.1007/s00170-020-04946-2.

[45] K. Derekar, J. Lawrence, G. Melton, A. Addison, X. Zhang, and L. Xu, “Influence of Interpass Temperature on Wire Arc Additive Manufacturing (WAAM) of Aluminium Alloy Components,” *MATEC Web of Conferences*, vol. 269, p. 05001, Feb. 2019, doi: 10.1051/matecconf/201926905001.

[46] W. Hackenhaar, J. A. E. Mazzaferro, F. Montevecchi, and G. Campatelli, “An experimental-numerical study of active cooling in wire arc additive manufacturing,” *Journal of Manufacturing Processes*, vol. 52, no. October 2019, pp. 58–65, Apr. 2020, doi: 10.1016/j.jmapro.2020.01.051.

[47] Y. Zhao, Y. Jia, S. Chen, J. Shi, and F. Li, “Process planning strategy for wire-arc additive manufacturing : Thermal behavior considerations,” *Additive Manufacturing*, vol. 32, no. September 2019, p. 100935, 2020, doi: 10.1016/j.addma.2019.100935.

[48] W. Chen, Y. Chen, T. Zhang, T. Wen, Z. Yin, and X. Feng, “Effect of Ultrasonic Vibration and Interpass Temperature on Microstructure and Mechanical Properties of Cu-8Al-2Ni-2Fe-2Mn Alloy Fabricated by Wire Arc Additive Manufacturing,” *Metals*, vol. 10, no. 2, p. 215, Feb. 2020, doi: 10.3390/met10020215.

[49] S. Salahi, A. V. Nemani, M. Ghaffari, J. Lunde, and A. Nasiri, “On microstructure, crystallographic orientation, and corrosion properties of wire arc additive manufactured 420 martensitic stainless steel: Effect of the inter-layer temperature,” *Additive Manufacturing*, vol. 46, no. January, p. 102157, Oct. 2021, doi: 10.1016/j.addma.2021.102157.

[50] J. Müller, J. Hensel, and K. Dilger, “Mechanical properties of wire and arc additively

manufactured high-strength steel structures," *Welding in the World*, vol. 66, no. 3, pp. 395–407, 2022, doi: 10.1007/s40194-021-01204-1.

[51] C. R. Cunningham, V. Dhokia, A. Shokrani, and S. T. Newman, "Effects of in-process LN2 cooling on the microstructure and mechanical properties of type 316L stainless steel produced by wire arc directed energy deposition," *Materials Letters*, vol. 282, p. 128707, Jan. 2021, doi: 10.1016/j.matlet.2020.128707.

[52] C. Shen *et al.*, "Effect of the post-production heat treatment on phase evolution in the Fe3Ni–FeNi functionally graded material: An in-situ neutron diffraction study," *Intermetallics*, vol. 129, no. August 2020, p. 107032, Feb. 2021, doi: 10.1016/j.intermet.2020.107032.

[53] R. Scharf-Wildenhain, A. Haelsig, J. Hensel, K. Wandtke, D. Schroepfer, and T. Kannengiesser, "Heat control and design-related effects on the properties and welding stresses in WAAM components of high-strength structural steels," *Welding in the World*, no. 0123456789, 2022, doi: 10.1007/s40194-022-01450-x.

[54] S. Prathivraj and R. Oyyaravelu, "Effect of interpass temperature on austenite ferrite ratio of wire arc additive manufactured 2507 Super Duplex Stainless Steel," *Materials Letters*, vol. 361, no. December 2023, p. 136125, 2024, doi: 10.1016/j.matlet.2024.136125.

[55] S. P. Yu and J. S. Jhong, "Optimization of surface roughness in WAAM-fabricated ER70S-6 steel components," *Materials Letters*, vol. 399, no. June, p. 139024, 2025, doi: 10.1016/j.matlet.2025.139024.

[56] M. Li *et al.*, "Effect of the interlayer temperature on microstructure and mechanical behavior of the high-strength low-alloy steel manufactured by the wire arc additive manufacturing," *Materials Today Communications*, vol. 46, no. May, p. 112845, Jun. 2025, doi: 10.1016/j.mtcomm.2025.112845.

[57] G. H. S. F. L. Carvalho and G. Campatelli, "Control of interpass temperature and arc oscillation for improved mechanical properties and geometrical uniformity in Ti6Al4V alloy deposition using wire arc additive manufacturing," *The International Journal of Advanced Manufacturing Technology*, vol. 136, no. 11–12, pp. 5025–5041, Feb. 2025, doi: 10.1007/s00170-025-15106-9.

[58] K. Wang, Y. Liu, Z. Sun, J. Lin, Y. Lv, and B. Xu, "Microstructural evolution and mechanical properties of Inconel 718 superalloy thin wall fabricated by pulsed plasma arc additive manufacturing," *Journal of Alloys and Compounds*, vol. 819, p. 152936, Apr. 2020, doi: 10.1016/j.jallcom.2019.152936.

[59] A. Vahedi Nemani, M. Ghaffari, and A. Nasiri, "On the Post-Printing Heat Treatment of a Wire Arc Additively Manufactured ER70S Part," *Materials*, vol. 13, no. 12, p. 2795, Jun. 2020, doi: 10.3390/ma13122795.

[60] C. Zhang, Y. Li, M. Gao, and X. Zeng, "Wire arc additive manufacturing of Al-6Mg alloy using variable polarity cold metal transfer arc as power source," *Materials Science and Engineering: A*, vol. 711, no. November 2017, pp. 415–423, Jan. 2018, doi: 10.1016/j.msea.2017.11.084.

[61] J. Du, G. Zhao, and Z. Wei, "Effects of Welding Speed and Pulse Frequency on Surface Depression in Variable Polarity Gas Tungsten Arc Welding of Aluminum Alloy," *Metals*, vol. 9, no. 2, p. 114, Jan. 2019, doi: 10.3390/met9020114.

[62] T. A. Rodrigues, V. Duarte, R. M. Miranda, T. G. Santos, and J. P. Oliveira, "Current Status and Perspectives on Wire and Arc Additive Manufacturing (WAAM)," *Materials*, vol. 12, no. 7, p. 1121, Apr. 2019, doi: 10.3390/ma12071121.

[63] T. Hauser *et al.*, "Porosity in wire arc additive manufacturing of aluminium alloys," *Additive Manufacturing*, vol. 41, no. April, p. 101993, May 2021, doi: 10.1016/j.addma.2021.101993.

[64] B. Cong, Z. Qi, B. Qi, H. Sun, G. Zhao, and J. Ding, "A Comparative Study of Additively Manufactured Thin Wall and Block Structure with Al-6.3%Cu Alloy Using Cold Metal Transfer Process," *Applied Sciences*, vol. 7, no. 3, p. 275, Mar. 2017, doi: 10.3390/app7030275.

[65] J. Gu, S. Yang, M. Gao, J. Bai, Y. Zhai, and J. Ding, "Micropore evolution in additively manufactured aluminum alloys under heat treatment and inter-layer rolling," *Materials & Design*, vol. 186, p. 108288, Jan. 2020, doi: 10.1016/j.matdes.2019.108288.

[66] Z. Wang and Y. Zhang, "A review of aluminum alloy fabricated by different processes of wire arc additive manufacturing," *Medziagotyra*, vol. 27, no. 1, pp. 18–26, 2021, doi: 10.5755/j02.ms.22772.